Hindawi
Journal of Chemistry
Volume 2019, Article ID 5036019, 9 pages
https://doi.org/10.1155/2019/5036019

Research Article

Study on the Photodegradation Stability of Poly(butylene Succinate-*co*-butylene Adipate)/TiO_2 Nanocomposites

Lihai Cai, Zhiguo Qi, Jun Xu, Baohua Guo, and Zhongyao Huang

Key Laboratory of Advanced Materials of Ministry of Education, Department of Chemical Engineering, Tsinghua University, Beijing 100084, China

Correspondence should be addressed to Baohua Guo; bhguo@mail.tsinghua.edu.cn

Received 2 December 2018; Revised 17 January 2019; Accepted 29 January 2019; Published 3 March 2019

Academic Editor: Leonardo Palmisano

Copyright © 2019 Lihai Cai et al. This is an open access article distributed under the Creative Commons Attribution License, which permits unrestricted use, distribution, and reproduction in any medium, provided the original work is properly cited.

A poly(butylene succinate-co-butylene adipate)/TiO_2 (PBSA/TiO_2) nanocomposite was prepared by a melt-blending process. The effect of TiO_2 nanoparticles on the photodegradation behaviors of the nanocomposite was investigated by transmission electron microscopy (TEM), differential scanning calorimetry (DSC), Fourier-transform infrared spectroscopy (FT-IR), field-emission scanning electron microscopy (FE-SEM), rheological measurements, and mechanical tests. TEM images of the PBSA/TiO_2 revealed that the TiO_2 nanoparticles were well dispersed in the matrix without obvious aggregation. The FT-IR results indicated that the TiO_2 nanoparticles can block high-energy ultraviolet (UV) light and reduce the degradation of the PBSA matrix. The viscosity analysis results indicated that the TiO_2 nanoparticles inhibited the chain scission of PBSA matrix under irradiation. In addition, the surface of the PBSA/TiO_2 films and their mechanical properties change less than that of untreated PBSA films during the photoaging process. The obtained results imply that the TiO_2 nanoparticles can be considered as an efficient photodegradation-resistant additive to PBSA for reducing photodegradation.

1. Introduction

Biodegradable polymers have gained significant attention because of their potential to alleviate certain environmental problems [1, 2]. Specifically, poly(butylene succinate) (PBS) and copolymer poly(butylene succinate-co-butylene adipate) (PBSA) are very attractive for their mechanical properties and service temperatures, which are even comparable with current polyolefin materials [2]. At present, these chemicals can find applications in packaging materials, biodegradable fibers, injection-molded products, mulch films, and other areas [3, 4]. Unfortunately, an insufficient service life limits this material's further applications, as it is easy to become fragile during storage, transportation, and outdoor use by exposure to heat, oxygen, and ultraviolet (UV) light [5]. As reported by Konstantinou and Albanis [6], the service environment is the cause of oxidation and loss or breakage of small molecular components, which eventually leads to the poor physical properties of PBSA.

As the stability of the mechanical properties during the aging process is important for extending service life, many researchers have attempted to reduce any change in the physical properties of PBS over time, such as chemical copolymerization, physical blending, and nanocompounding [2, 7–9]. However, there is little research on improving the stability of PBSA's mechanical properties during the photoaging process.

Yang et al. [10] used SiO_2, Al_2O_3, and ZnO nanoparticles as inhibitors on linear low-density polyethylene (LLDPE) and compared three kinds of composites to the pure LLDPE after irradiation. The results showed that all three types of nanoparticles improved the photodegradation stability of the resulting nanocomposites. Huang et al. [11] prepared PBS/TiO_2 nanocomposites via a vane extruder and found that the introduction of TiO_2 improved the thermal stability and mechanical properties stability of the nanocomposites. Yang et al. [12] studied the UV-blocking property of TiO_2 powders with different-sized additives for films and fabrics, showing that TiO_2 is a good UV-barrier-additive for polymer matrices due to their properties of UV absorption, scattering, and reflection.

In the studies mentioned [10–19], the TiO_2 nanoadditives have attracted a high degree of attention, mainly

because they are not only UV-screening agents but also performance-enhancing additives. Furthermore, as TiO_2 is more refractive than that of most light-colored inorganic additives, such as SiO_2, Al_2O_3, ZnO, and others, the ability of shielding UV radiation is stronger than that of other additives [20].

The purpose of this paper was to improve the photodegradation stability and prolong the service life of PBSA by adding nano-TiO_2 additives based on their UV-screening characteristics. The different TiO_2 loadings of PBSA/TiO_2 nanocomposites were prepared by a melt-blending process. The effect of the TiO_2 nanoparticles on the photodegradation behaviors of the nanocomposite was investigated by transmission electron microscopy (TEM), differential scanning calorimetry (DSC), Fourier-transform infrared spectroscopy (FT-IR), scanning electron microscopy (SEM), rheological measurements, and mechanical tests.

2. Experimental

2.1. Materials. The PBSA pellets were supplied by Blue Ridge Tunhe Polyester Co., Ltd. (China). The comonomer content of the adipic acid used for PBSA was set at 5 mol%. The index of the melt flow was 16.1 g per 10 min. The melting temperature was 111.9°C. Rutile TiO_2 nanoparticles coated with silicon-aluminum composite compounds were supplied by Hangzhou Wanjing New Material Co., Ltd. (China).

2.2. PBSA/TiO_2 Nanocomposite Preparation. The PBSA-added nano-TiO_2 (PBSA/TiO_2) nanocomposites were prepared by melt compounding by an RS600 HAAKE mixer. The speed of the rotary was 40–60 rpm, and the mixing temperature was 140°C. When preparing the PBSA/TiO_2 nanocomposite with 0.1 wt.% TiO_2, 49.95 g of PBSA pellets was first fed into a mixing chamber and blended for 2 min at 140°C. Then, 0.05 g of TiO_2 nanoparticles were added to the chamber and blended for another 10 min. PBSA/TiO_2 nanocomposites containing 0.5, 1.0, and 1.5 wt.% TiO_2 were prepared according to the proportional relation. The pure PBSA pellets were also blended in the mixing chamber for 2 min at 140°C. The films and plates of the pure PBSA and PBSA/TiO_2 nanocomposites were molded by hot-pressing. The thicknesses of the film samples and plate samples were about 100 μm and 2 mm, respectively.

2.3. Photoaging Test. The film and plate samples with different TiO_2 contents were exposed to the aging chamber for accelerated photoaging tests. The aging test of the samples was carried out at 38 ± 2°C in a Q-SUN xenon test chamber (Xe-3-HS, Q-Lab Co., USA) for different times. The energy distribution in the test chamber simulated that of the solar spectrum, and the relative humidity in the chamber was 30 ± 5%.

2.4. Morphology Characterization. The surface morphology of film samples was observed by SEM (JSM-7401, Japan). The SEM samples were plated with platinum before observation at a scan voltage of 3 kV. The dispersion of TiO_2 nanoparticles in the PBSA matrix was observed by TEM (JEOL JEM-2000) at a voltage of 120 kV. The TEM samples were prepared with a microtome (Leica EMUC 6, Germany) at −80°C, and the samples were placed on copper grids.

2.5. Carbonyl Index Determination. The FT-IR spectra of the film samples were analyzed by an FT-IR spectrometer (Nicolet-6700, USA) with a Ge-attenuated total reflection detector. The wavenumber range was from 400 to 4000 cm^{-1} by signal averaging 32 scans at a resolution of 4 cm^{-1}. The carbonyl index ($A_{C=O}/A_{C-H}$) was defined as the area ratio of carbonyl absorbance to the reference peak [21–23], and the changes in the carbonyl absorbance are represented in detail in the region of 1600–1800 cm^{-1}. The 2856 cm^{-1} peak was attributed to the C–H stretching according to the previous literature [24].

2.6. Viscosity Aging Index Determination. The dynamic rheology of the plate samples was measured by a stress-/strain-controlled rheometer (Anton Paar MCR301) [25, 26]. The diameter of the rheometer parallel plate was 25 mm, and the testing gap was 1 mm. The oscillatory shear model was used in the rheological tests with parameters set at a temperature of 140°C, a deformation strain of 1%, and a sweep frequency range from 0.01 to 100 Hz. In order to compare the decrease of the zero-shear viscosity of samples after irritation, the viscosity aging index (VAI) was introduced according to the following formula:

$$\mathrm{VAI} = \frac{|\eta_0^*| - |\eta_t^*|}{|\eta_0^*|} \times 100\%, \quad (1)$$

where $|\eta_0^*|$ is the initial viscosity value, with the data read from the curves of complex viscosity at 0.01 Hz of samples, and $|\eta_t^*|$ is the aged viscosity value.

2.7. Thermal Analysis. The thermal behavior of the film samples was tested by a differential thermal analyzer (Shimadzu DSC-60, Japan) at an N_2 flow of 50 mL/min. The samples (3–5 mg) were sealed in aluminum crucibles with an empty aluminum seal crucible as a reference. During the test, the sample was heated from 30 to 160°C then held for 5 min in order to eliminate the thermal history in the aging test; then the sample was cooled to 30°C. The rate of the heating and cooling operations was both 10°C/min. The crystallinity of PBSA/TiO_2 and pure PBSA nanocomposites was calculated with the following formula:

$$X_C = \frac{\Delta H_m}{(1-\omega)\Delta H_m^0} \times 100\%, \quad (2)$$

where ΔH_m is the melting enthalpy of the sample, ΔH_m^0 is the melting enthalpy of PBS that is 100% crystalline ($\Delta H_m^0 = 110.3$ J/g [27]), and ω is the content of TiO_2 in the PBSA matrix by weight percentage.

2.8. Mechanical Tests. The mechanical properties of the film samples were measured at $25 \pm 2^{\circ}$C by a TS-2000 tester (Gotech Inc., Taiwan), including tensile strength and elongation at break. The sample was conditioned in 30% relative humidity for 48 h at $25 \pm 2^{\circ}$C before testing. The rising speed of the crosshead was 10 mm/min. The final test results were calculated from the mean value of five measurements for each sample.

3. Results and Discussion

3.1. Dispersion of Nanoparticles in Polymer Matrix. Figure 1 shows a TEM image of PBSA/TiO_2 nanocomposites containing 1.5 wt.% TiO_2, from which it can be seen that the TiO_2 nanoparticles are dispersed evenly in the PBSA matrix without obvious aggregation, and the size of nanoparticles is from 30 to 50 nm. The good dispersion of TiO_2 in PBSA can be attributed to the surface modification by the coated compound [28] and the high sheer forces during extrusion, which reduced the aggregation of the nanoparticles.

3.2. FT-IR Characterization. The FT-IR spectra of pure PBSA was acquired; the peak in the 1046 cm^{-1} region is due to the stretching of the carbon-oxygen bond [29]. The 1157 cm^{-1} peak was assigned to the stretching of the carbon-oxygen-carbon group in the ester bond of PBSA [30]. The band region from 1650 to 1750 cm^{-1} results from C=O stretching of the ester group [29] and the degradation fragments [31]. The 2856 and 2946 cm^{-1} peaks were assigned to C–H stretching, and the peak at 2856 cm^{-1} peak was used as the reference in calculating the value of the carbonyl index [24].

Carroccio [32] investigated the photo-oxidation of poly(butylene succinate) by mass spectrometry and ascertained three photo-oxidation processes of aliphatic polyesters, including α-hydrogen abstraction, the Norrish I of chain cleavage, and the hydroxyl end groups oxidation. During the processes of photo-oxidation, many aldehyde and carboxyl groups were produced, and the content of carboxyl groups changed dynamically at different oxidation times (Scheme 1), which corresponds with the increase and broadening of C=O peaks with increasing irradiation, as seen in Figure 2. After further comparisons of the FT-IR curves for the PBSA/TiO_2 nanocomposite with pure PBSA under the same irradiation time in Figure 2, the increase of the C=O peak intensity for the PBSA/TiO_2 nanocomposite is less than that of pure PBSA, which indicates that the TiO_2 nanoparticles can significantly prevent the PBSA photodegradation process.

Normally, the carboxyl groups can be used as a signature to reveal the degree of photodegradation of PBSA [31]. Figure 3 shows the changes in the carbonyl index of the PBSA/TiO_2 nanocomposites and pure PBSA at different irradiation times. It can be seen that the photodegradation process starts immediately as the irradiation process starts [27]. The carbonyl index of the pure PBSA is higher than that of any PBSA/TiO_2 nanocomposite. With the increase of the TiO_2 content, the value of the carbonyl index decreases gradually at the same irradiation time. This means that TiO_2 is an effective stabilizer for PBSA under irradiation. The improvement in the photostability of PBSA with the nano-TiO_2 results from the fact that the rutile-type TiO_2 nanoparticles have strong absorbability within the UV band by the quantum size effect [11, 12], which can block high-energy UV light effectively and reduce photodegradation of the PBSA matrix.

3.3. Rheological Properties. The changes of molecular weight and the degradation degree of the polymer can be characterized by the change of viscosity [25, 26]. Figure 4 presents the complex viscosity of the PBSA/TiO_2 nanocomposites and pure PBSA both before and after 360 h of irradiation. All samples exhibit a non-Newtonian behavior in the entire frequency range of the rheological test and show the characteristic of shear thinning. The zero-shear viscosities of all nanocomposites are higher than that of pure PBSA, while the complex viscosity ($|\eta^*|$) of all nanocomposites decreases more rapidly than that of pure PBSA with the increase of frequency, demonstrating a much stronger shear thinning behavior [24].

Figure 4(a) shows the complex viscosity, ($|\eta^*|$), measured at 140°C as a function of the frequency before irradiation. The addition of nanoparticles leads to a significant increase in the viscosity at low shear rates. Similar behaviors have been previously observed for other nanocomposites [33, 34], with the reason behind the behavior being that TiO_2 can act as a physical entanglement point and improve the complex viscosity of PBSA at low frequencies. The formation of physical entanglement points in polymers results in the stress transfer between matrix and filler, which is beneficial to the improvement of mechanical properties, such as the tensile modulus and yield strength [34, 35].

After irradiation, it can be seen that there was an obvious reduction of the zero-shear viscosity in the samples after 360 h of irradiation when compared to the initial samples (Figure 4(b)). As reported previously [36, 37], there is a power law relationship between the molecular weight and the zero-shear viscosity of linear polymers. Corresponding to the Norrish I reaction of the photo-oxidation processes in Scheme 1, the decrease of the zero-shear viscosity indicates that the photodegradation of PBSA provokes chain scission; then the low-molecular-weight products have been formed by degradation [38]. Table 1 lists the VAI values of pure PBSA and the PBSA/TiO_2 nanocomposites after 360 h of irradiation. The VAI value of pure PBSA is as large as 89.3%, and the value decreases with the increase of TiO_2 in the matrix of the PBSA/TiO_2 nanocomposites, which results from the positive effect of TiO_2 during the photoaging process.

3.4. Thermal Properties. The thermal properties of the samples for different irradiation times were detected by DSC. The crystallization temperature (T_c) and melting temperature (T_m) were obtained by reading the peak values of cooling curves and heating curves, respectively. The crystallinity was calculated from the DSC curves.

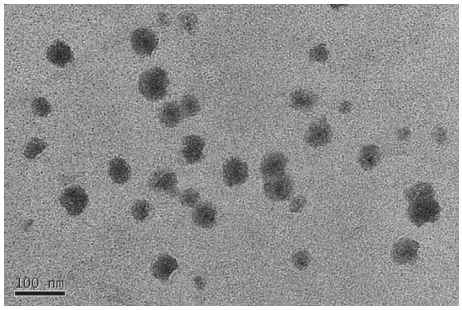

Figure 1: TEM image of PBSA containing 1.5 wt.% TiO_2 at a magnification of 50 kX.

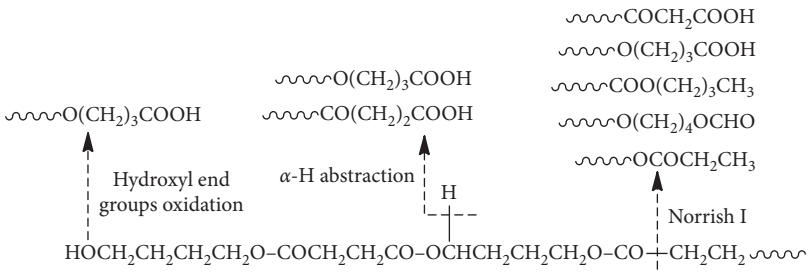

Scheme 1: Overall photo-oxidation processes in PBS and its copolymers [32].

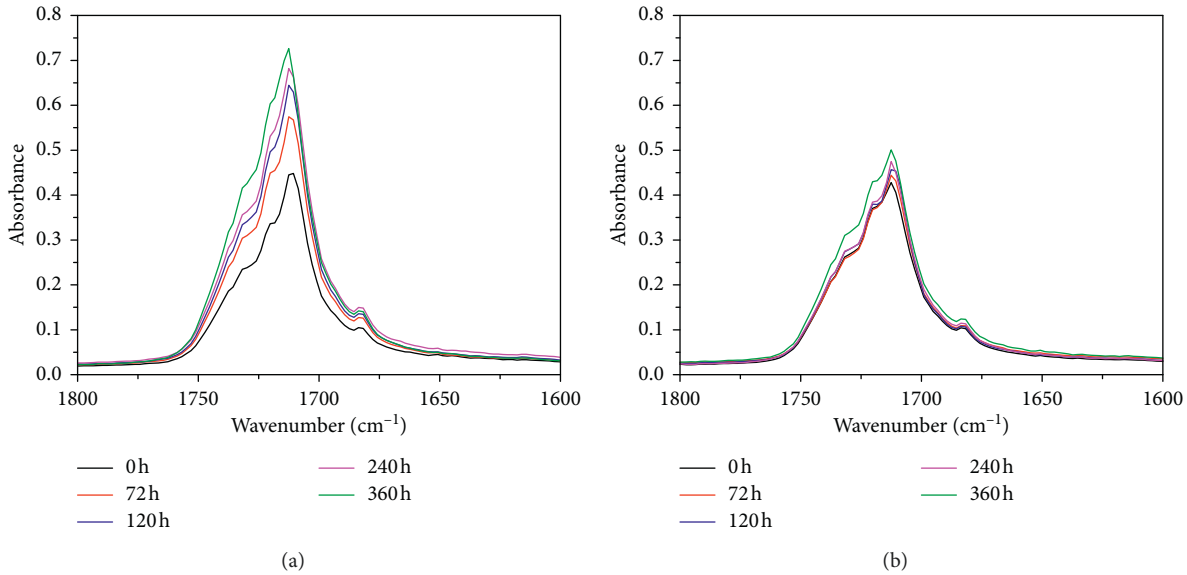

Figure 2: FT-IR spectra of (a) pure PBSA and (b) PBSA/TiO_2 nanocomposites containing 1.5 wt.% TiO_2 at different irradiation times.

Figure 5 shows the change of T_c and crystallinity of the PBSA/TiO_2 nanocomposites and pure PBSA both before irradiation and after being irradiated for 72, 120, 240, and 360 h. For the unaged samples, it can be seen that the T_c and crystallinity of pure PBSA are the smallest. With the increase of TiO_2 content in the PBSA/TiO_2 nanocomposites, the T_c and crystallinity increase gradually. The relationship between both the test parameters of the samples and the TiO_2 content shows that TiO_2 is beneficial for promoting the nucleation and crystallization of PBSA, which was also reported by Zhou et al. [39].

From the data in Table 2, the T_m of all samples show few differences after 360 h of irradiation. However, the T_c decreases, and the crystallinity increases significantly after 360 h of irradiation. Furthermore, the pure PBSA showed the largest decrease in T_c and the maximum increase in crystallinity. The decrease in T_c can be attributed to some long chains of PBSA breaking during UV irradiation with the broken short chains having stronger mobility, which is helpful for ordering shorter chains at lower temperature and reducing the crystallization temperature [23]. In addition, the higher mobility of the broken molecules in the

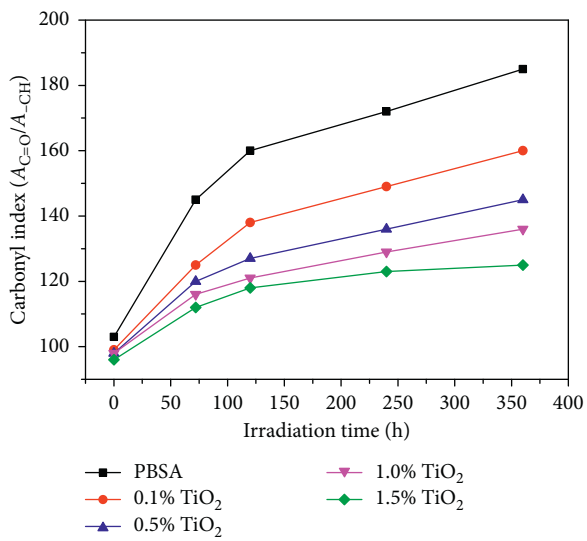

Figure 3: Changes in the carbonyl index of PBSA/TiO_2 nanocomposites and pure PBSA at different irradiation times.

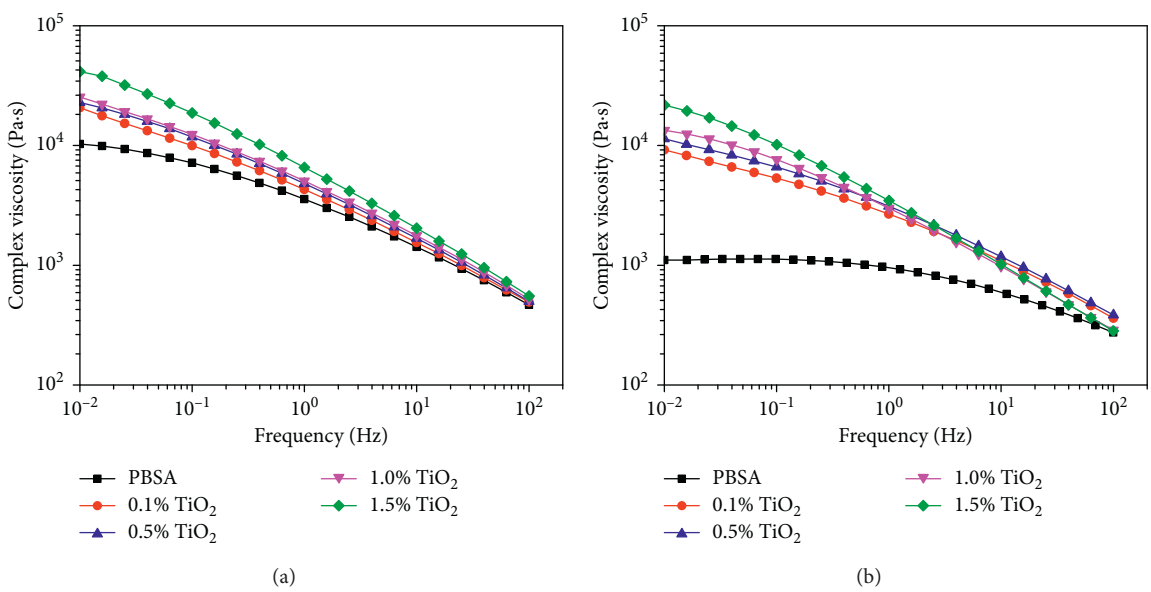

Figure 4: Complex viscosity of pure PBSA and PBSA/TiO_2 nanocomposites (a) before and (b) after 360 h of UV irradiation as a function of frequency at 140°C.

Table 1: VAI values of PBSA/TiO_2 nanocomposites before and after 360 h of UV irradiation.

TiO_2 (%)	$\lvert\eta^*\rvert_{0\,h}$ ($P_a \cdot s$)	$\lvert\eta^*\rvert_{360\,h}$ ($P_a \cdot s$)	VAI (%)
0	10300	1105	89.3
0.1	20700	9200	55.6
0.5	22900	11400	50.2
1.0	25400	14470	43.0
1.5	41500	25430	38.7

amorphous regions can cause them to rearrange and recrystallize, which promotes the increase of crystallinity [40]. As the TiO_2 content increases in pure PBSA, the degradation of the PBSA chains decreases gradually, and the effect of the degraded shorter chains on reducing the crystallization temperature and promoting crystallization is weakened accordingly.

3.5. Surface Morphology. The morphological changes caused by irradiation were analyzed by SEM to reveal the effect of surface changes on the photodegradation. Figure 6 shows the surface changes of PBSA/TiO_2 nanocomposites and pure PBSA film both before and after 360 h of irradiation at a magnification of 3 kX. Before irradiation, both the PBSA/TiO_2 nanocomposites and pure PBSA film exhibit a relatively smooth surface.

The surface of the pure PBSA film becomes rough with randomly distributed pores appearing after 360 h of

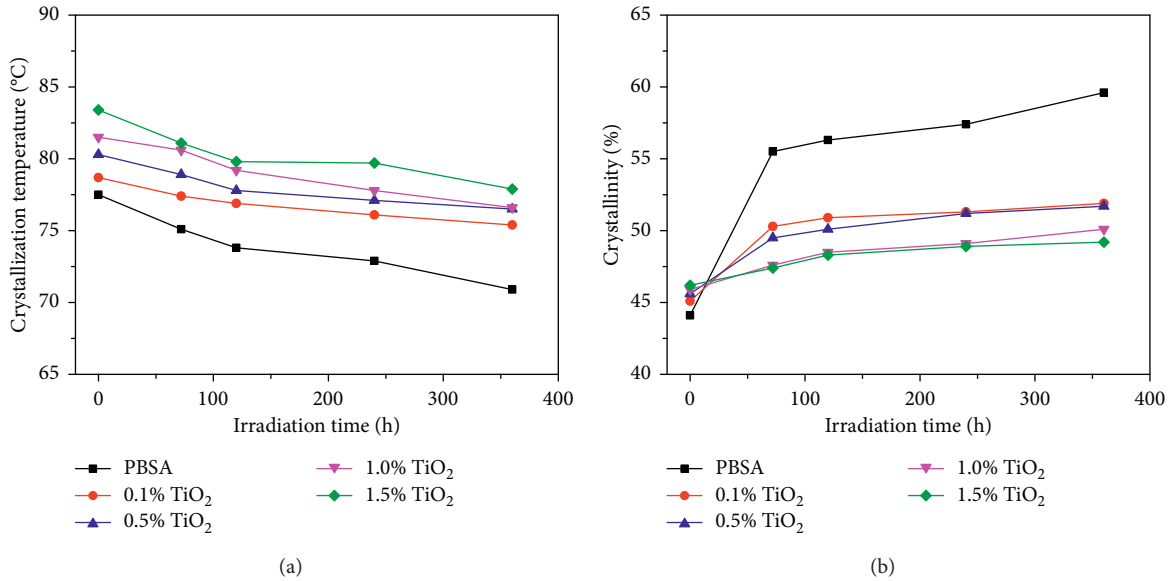

Figure 5: (a) Crystallization temperature and (b) crystallinity of PBSA/TiO_2 nanocomposites and pure PBSA as a function of irradiation time.

Table 2: Thermal parameters of PBSA/TiO_2 nanocomposites with and without irradiation time.

TiO_2 (%)	Irradiation time (h)	T_m (°C)	T_c (°C)	X_c (%)
0	0	111.5	77.5	44.1
0.1	0	111.3	78.7	45.1
0.5	0	111.6	80.3	45.6
1.0	0	111.4	81.5	45.9
1.5	0	111.5	83.4	46.2
0	360	111.7	70.9	59.6
0.1	360	111.5	75.4	51.9
0.5	360	111.7	76.5	51.7
1.0	360	111.4	76.6	50.1
1.5	360	111.7	77.9	49.2

irradiation, which is consistent with the observations by Zhang et al. [23]. The formation of the pores is due to the degradation of the PBSA, beginning from the film surface, and then deteriorating in the depth dimension with irradiation time. In contrast, the surface of the PBSA/TiO_2 film changes little under the same irradiation conditions, which shows that the TiO_2 nanoparticles can effectively delay the aging of the PBSA matrix.

3.6. Mechanical Properties. Figure 7 shows the mechanical properties of film samples for different irradiation times. For the pure PBSA film, the tensile strength is 16.6 MPa, the elongation at break is 431%, and both mechanical parameters obviously decreased with the increase of irradiation time. For the unaged samples containing TiO_2 nanoparticles, the tensile strength increased, and the elongation decreased compared to pure PBSA (Figure 7(a)). As the irradiation time increased, the elongation of PBSA/TiO_2 nanocomposites decreased gradually, and the strength changed slowly. As can be seen from Figure 7(b), as the aging time increases, the elongation at break of the pure PBSA decreases from 420% to 250%, while that of nanocomposites containing 1.5% TiO_2 decreases from 337% to 302%. The changing trend of elongation at break after irradiation is similar to that of VAI in the rheological test in Table 1, which indicates that nano-TiO_2 can effectively prevent the breaking of molecular chains as the elongation at break has correlation with molecular weight, and it has a positive effect on maintaining the mechanical properties during irradiation.

4. Conclusion

In this study, rutile TiO_2 nanoparticles were mixed with PBSA, and the PBSA/TiO_2 nanocomposites were successfully prepared by melt-blending. The effect of the TiO_2 nanoparticles on the photodegradation behaviors of the nanocomposites was investigated. The changes in the carbonyl index analysis, thermal properties, and rheological properties of the pure PBSA were caused by chain cleavage and group oxidation under the photoaging process, which spurred the surface of the sample until it was rough and worsened its mechanical properties. The rutile-type TiO_2 nanoparticles, well dispersed in the matrix, can retard the chain scission of

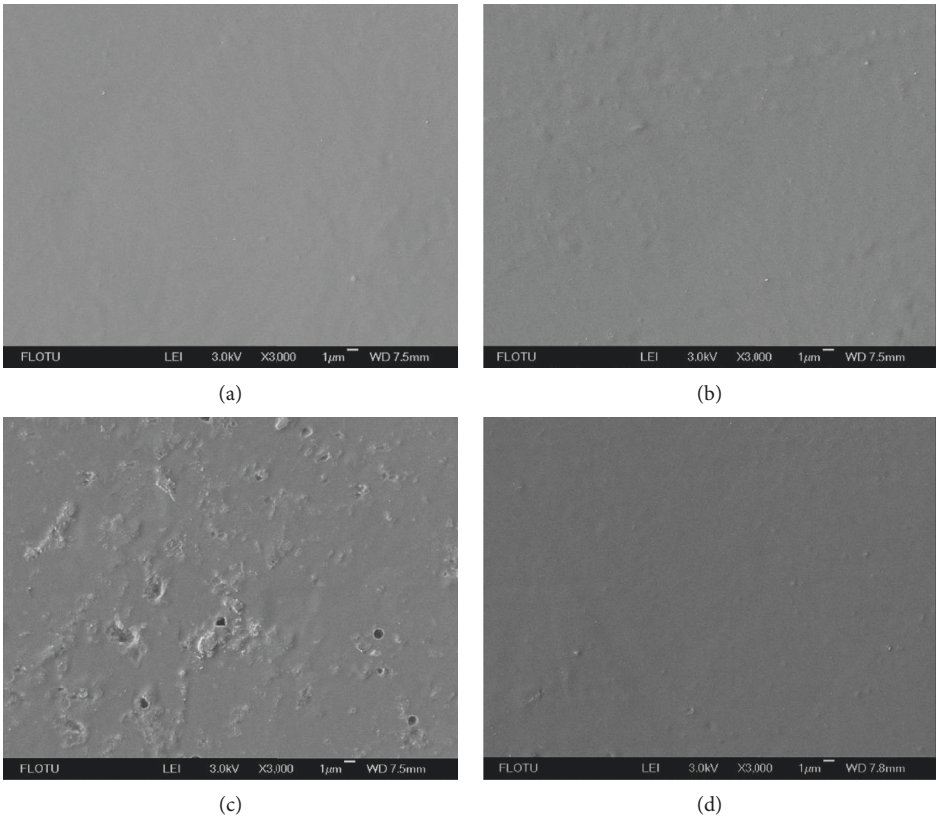

Figure 6: SEM images of surface changes before UV irradiation of (a) pure PBSA and (b) PBSA containing 1.5 wt.% TiO_2 and after 360 h UV irradiation of (c) pure PBSA and (d) PBSA containing 1.5 wt.% TiO_2 at a magnification of 3 kX.

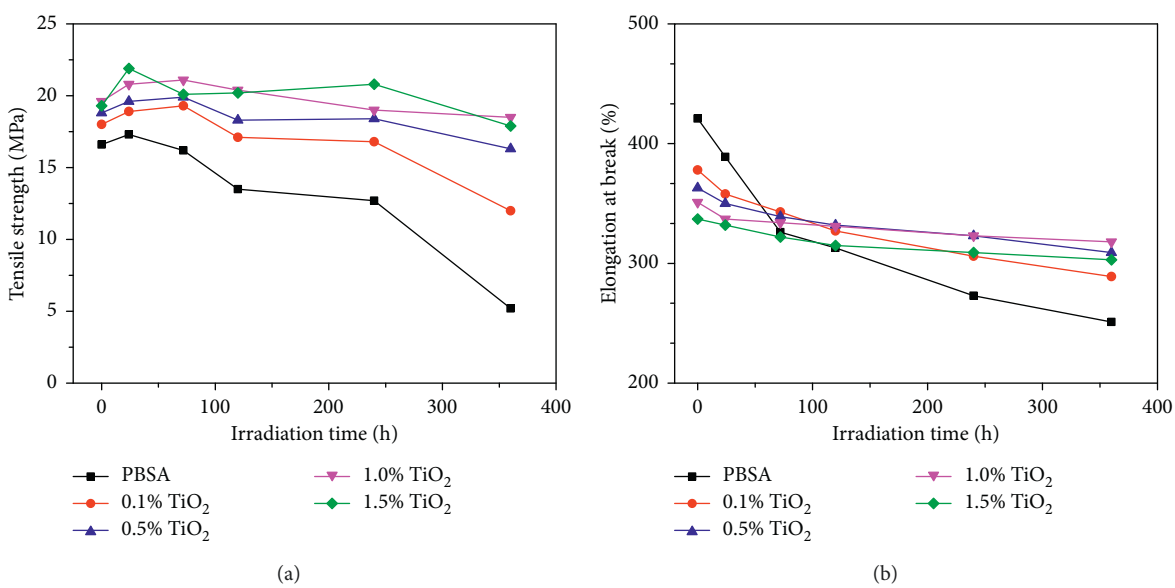

Figure 7: (a) Tensile strength and (b) elongation at the break of PBSA/TiO_2 and pure PBSA films as a function of irradiation time.

PBSA, which effectively improves the surface integrity and mechanical properties of the nanocomposites under irradiation. This study may promote the application of PBSA in the industry and improve its service life.

Data Availability

The compressed data named DATA.rar used to support the findings of this study have been deposited in the Figshare

repository, and the link is https://figshare.com/s/b00ca17289a252f90acd.

Conflicts of Interest

The authors declare that there are no conflicts of interest regarding the publication of this paper.

Acknowledgments

The authors thank the National Natural Science Foundation of China (Grant nos. 51673110 and 51473085), the Joint Funds of the National Natural Science Foundation of China (Grant no. U1862205), and the Tsinghua University-Suzhou Innovation Leading Program (Grant no. 20172140200) for the financial support in this work.

References

[1] M. M. Reddy, S. Vivekanandhan, M. Misra, S. K. Bhatia, and A. K. Mohanty, "Biobased plastics and bionanocomposites: current status and future opportunities," *Progress in Polymer Science*, vol. 38, no. 10–12, pp. 1653–1689, 2013.

[2] J. Xu and B.-H. Guo, "Poly(butylene succinate) and its copolymers: research, development and industrialization," *Biotechnology Journal*, vol. 5, no. 11, pp. 1149–1163, 2010.

[3] S. S. Ray, M. Bousmina, and K. Okamoto, "Structure and properties of nanocomposites based on poly(butylene succinate-co-adipate) and organically modified montmorillonite," *Macromolecular Materials and Engineering*, vol. 290, no. 8, pp. 759–768, 2005.

[4] J. A. Ratto, P. J. Stenhouse, M. Auerbach, J. Mitchell, and R. Farrell, "Processing, performance and biodegradability of a thermoplastic aliphatic polyester/starch system," *Polymer*, vol. 40, no. 24, pp. 6777–6788, 1999.

[5] H. Zhang, J. Yu, H. Wang, and L. Xue, "Investigation of microstructures and ultraviolet aging properties of organo-montmorillonite/SBS modified bitumen," *Materials Chemistry and Physics*, vol. 129, no. 3, pp. 769–776, 2011.

[6] I. K. Konstantinou and T. A. Albanis, "TiO_2-assisted photocatalytic degradation of azo dyes in aqueous solution: kinetic and mechanistic investigations," *Applied Catalysis B: Environmental*, vol. 49, no. 1, pp. 1–14, 2004.

[7] J. Du, Y. Zheng, and L. Xu, "Biodegradable liquid crystalline aromatic/aliphatic copolyesters. Part I: synthesis, characterization, and hydrolytic degradation of poly(butylene succinate-co-butylene terephthaloyldioxy dibenzoates)," *Polymer Degradation and Stability*, vol. 91, no. 12, pp. 3281–3288, 2006.

[8] H.-S. Kim, G.-X. Chen, H.-J. Jin, and J.-S. Yoon, "In situ copolymerization of butylene succinate with twice functionalized organoclay: thermal stability," *Colloids and Surfaces A: Physicochemical and Engineering Aspects*, vol. 313-314, pp. 56–59, 2008.

[9] S. S. Ray, "Visualisation of nanoclay dispersion in polymer matrix by high resolution electron microscopy combined with electron tomography," *Macromolecular Materials and Engineering*, vol. 294, no. 4, pp. 281–286, 2009.

[10] R. Yang, Y. Li, and J. Yu, "Photo-stabilization of linear low density polyethylene by inorganic nano-particles," *Polymer Degradation and Stability*, vol. 88, no. 2, pp. 168–174, 2005.

[11] J. Huang, X. Lu, N. Zhang et al., "Study on the properties of nano-TiO_2/polybutylene succinate composites prepared by vane extruder," *Polymer Composites*, vol. 35, no. 1, pp. 4360–4365, 2014.

[12] H. Yang, S. Zhu, and N. Pan, "Studying the mechanisms of titanium dioxide as ultraviolet-blocking additive for films and fabrics by an improved scheme," *Journal of Applied Polymer Science*, vol. 92, no. 5, pp. 3201–3210, 2004.

[13] H. Zhao and R. K. Y. Li, "A study on the photo-degradation of zinc oxide (ZnO) filled polypropylene nanocomposites," *Polymer*, vol. 47, no. 9, pp. 3207–3217, 2006.

[14] O. H. Lin, H. M. Akil, and S. Mahmud, "Effect of particle morphology on the properties of polypropylene/nanometric zinc oxide composites," *Advanced Composites Letters*, vol. 18, no. 3, pp. 77–83, 2009.

[15] S. Chandramouleeswaran, S. T. Mhaske, A. A. Kathe, P. V. Varadarajan, V. Prasad, and N. Vigneshwaran, "Functional behaviour of polypropylene/ZnO-soluble starch nanocomposites," *Nanotechnology*, vol. 18, no. 3, p. 385702, 2007.

[16] J. He, W. Shao, L. Zhang, C. Deng, and C. Li, "Crystallization behavior and UV-protection property of PET-ZnO nanocomposites prepared byin situpolymerization," *Journal of Applied Polymer Science*, vol. 114, no. 2, pp. 1303–1311, 2009.

[17] M. Miyauchi, Y. Li, and H. Shimizu, "Enhanced degradation in nanocomposites of TiO_2 and biodegradable polymer," *Environmental Science & Technology*, vol. 42, no. 12, pp. 4551–4554, 2008.

[18] Y. Zhang, M. Chen, and L. Wu, "Fabrication method of TiO_2–SiO_2 hybrid capsules and their UV-protective property," *Colloids and Surfaces A: Physicochemical and Engineering Aspects*, vol. 353, no. 2-3, 2010.

[19] R. Manna, S. Nayak, M. Rahaman, and D. Khastgir, "Effect of annealed titania on dielectric and mechanical properties of ethylene propylene diene monomer-titania nanocomposites," *E-Polymers*, vol. 14, no. 4, pp. 267–275, 2014.

[20] T. J. Kemp and R. A. McIntyre, "Mechanism of action of titanium dioxide pigment in the photodegredation of poly(vinyl chloride) and other polymers," *Progress in Reaction Kinetics and Mechanism*, vol. 26, no. 4, pp. 337–374, 2001.

[21] L.-H. Cai, Z.-G. Qi, J. Xu, B.-H. Guo, and Z.-Y. Huang, "Thermo-oxidative degradation of nylon 1010 films: colorimetric evaluation and its correlation with material properties," *Chinese Chemical Letters*, vol. 28, no. 5, pp. 949–954, 2017.

[22] T. K. N. Nguyen, H. G. Kim, L. K. Kwac, Q. B. Bui, D. M. Nguyen, and H. Jeong, "Titanium dioxide-benzophenone hybrid as an effective catalyst for enhanced photochemical degradation of low density polyethylene," *E-Polymers*, vol. 18, no. 6, pp. 501–510, 2018.

[23] Y. Zhang, J. Xu, and B. Guo, "Photodegradation behavior of poly(butylene succinate-co-butylene adipate)/ZnO nanocomposites," *Colloids and Surfaces A: Physicochemical and Engineering Aspects*, vol. 489, pp. 173–181, 2016.

[24] Z. Qi, H. Ye, J. Xu, J. Peng, J. Chen, and B. Guo, "Synthesis and characterizations of attapulgite reinforced branched poly(-butylene succinate) nanocomposites," *Colloids and Surfaces A: Physicochemical and Engineering Aspects*, vol. 436, pp. 26–33, 2013.

[25] S. J. Dalsin, M. A. Hillmyer, and F. S. Bates, "Molecular weight dependence of zero-shear viscosity in atactic polypropylene bottlebrush polymers," *ACS Macro Letters*, vol. 3, no. 5, pp. 423–427, 2014.

[26] D. Quemada, "Aging, rejuvenation and thixotropy in complex fluids. Time-dependence of the viscosity at rest and under

constant shear rate or shear stress," *Physics*, vol. 18, pp. 129–137, 2008.

[27] M. S. Nikolic and J. Djonlagic, "Synthesis and characterization of biodegradable poly(butylene succinate-co-butylene adipate)s," *Polymer Degradation and Stability*, vol. 74, no. 2, pp. 263–270, 2001.

[28] J. Godnjavec, J. Zabret, B. Znoj, S. Skale, N. Veronovski, and P. Venturini, "Investigation of surface modification of rutile TiO_2 nanoparticles with SiO_2/Al_2O_3 on the properties of polyacrylic composite coating," *Progress in Organic Coatings*, vol. 77, no. 1, pp. 47–52, 2014.

[29] H.-S. Kim, H.-J. Kim, J.-W. Lee, and I.-G. Choi, "Biodegradability of bio-flour filled biodegradable poly(butylene succinate) bio-composites in natural and compost soil," *Polymer Degradation and Stability*, vol. 91, no. 5, pp. 1117–1127, 2006.

[30] T. Uesaka, K. Nakane, S. Maeda, T. Ogihara, and N. Ogata, "Structure and physical properties of poly(butylene succinate)/cellulose acetate blends," *Polymer*, vol. 41, no. 23, pp. 8449–8454, 2000.

[31] T. Kijchavengkul, R. Auras, M. Rubino, S. Selke, M. Ngouajio, and R. T. Fernandez, "Biodegradation and hydrolysis rate of aliphatic aromatic polyester," *Polymer Degradation and Stability*, vol. 95, no. 12, pp. 2641–2647, 2010.

[32] S. Carroccio, P. Rizzarelli, C. Puglisi, and G. Montaudo, "MALDI investigation of photooxidation in aliphatic polyesters: poly(butylene succinate)," *Macromolecules*, vol. 37, no. 17, pp. 6576–6586, 2004.

[33] H. Eslami, M. Grmela, and M. Bousmina, "Linear and nonlinear rheology of polymer/layered silicate nanocomposites," *Journal of Rheology*, vol. 54, no. 3, pp. 539–562, 2010.

[34] S. S. Ray and M. Bousmina, "Poly(butylene sucinate-co-adipate)/montmorillonite nanocomposites: effect of organic modifier miscibility on structure, properties, and viscoelasticity," *Polymer*, vol. 46, no. 26, pp. 12430–12439, 2005.

[35] J. K. Mishra, K.-J. Hwang, and C.-S. Ha, "Preparation, mechanical and rheological properties of a thermoplastic polyolefin (TPO)/organoclay nanocomposite with reference to the effect of maleic anhydride modified polypropylene as a compatibilizer," *Polymer*, vol. 46, no. 6, pp. 1995–2002, 2005.

[36] T. G. Fox Jr. and P. J. Flory, "Further studies on the melt viscosity of polyisobutylene," *Journal of Physical Chemistry*, vol. 55, no. 2, pp. 221–234, 1951.

[37] R. H. Colby, L. J. Fetters, and W. W. Graessley, "The melt viscosity-molecular weight relationship for linear polymers," *Macromolecules*, vol. 20, no. 9, pp. 2226–2237, 1987.

[38] M. Gardette, S. Thérias, J.-L. Gardette, M. Murariu, and P. Dubois, "Photooxidation of polylactide/calcium sulphate composites," *Polymer Degradation and Stability*, vol. 96, no. 4, pp. 616–623, 2011.

[39] W. Zhou, T. Xu, X. Wang et al., "In situ polymerized nanocomposites of poly (butylene succinate)/TiO_2 nanofibers: molecular weight, morphology, and thermal properties," *Journal of Applied Polymer Science*, vol. 127, no. 1, pp. 733–739, 2012.

[40] A. Pegoretti and A. Penati, "Recycled poly(ethylene terephthalate) and its short glass fibres composites: effects of hygrothermal aging on the thermo-mechanical behaviour," *Polymer*, vol. 45, no. 23, pp. 7995–8004, 2004.

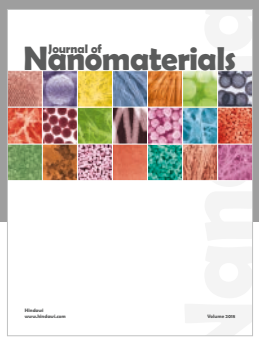

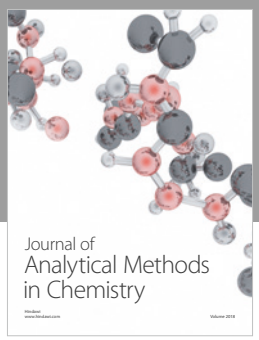

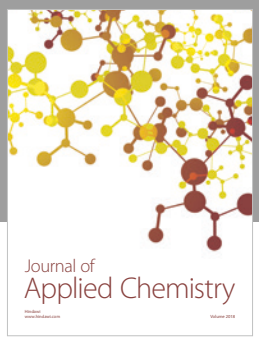

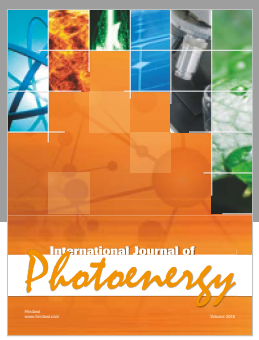

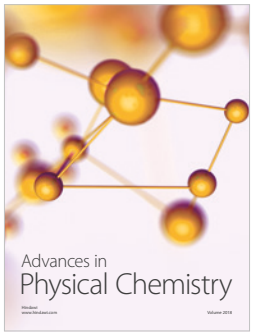

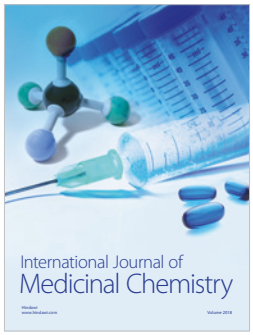

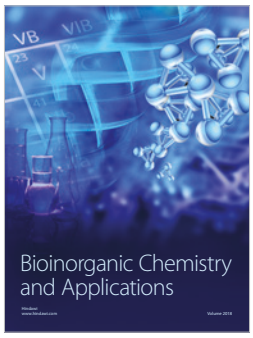

Hindawi
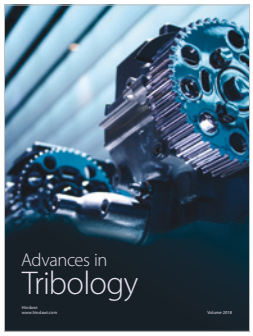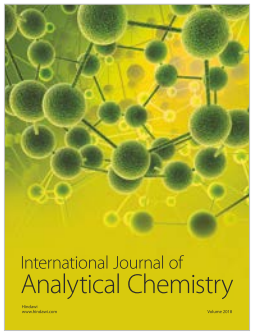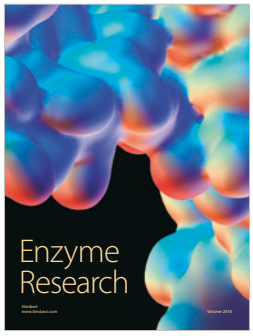
Submit your manuscripts at
www.hindawi.com